Baseline Connectome Modular Abnormalities in the Childhood Phase of a Longitudinal Study on Individuals With Chromosome 22q11.2 Deletion Syndrome

Liang Zhan,[1] Lisanne M. Jenkins,[2] Aifeng Zhang,[2] Giorgio Conte,[3] Angus Forbes,[3] Danielle Harvey,[4] Kathleen Angkustsiri,[10] Naomi J. Goodrich-Hunsaker,[5,6] Courtney Durdle,[5] Aaron Lee,[5] Cyndi Schumann,[5] Owen Carmichael,[7] Kristopher Kalish,[8] Alex D. Leow,[2,9]* and Tony J. Simon[5]*

[1]Computer Engineering Program, University of Wisconsin-Stout, Wisconsin
[2]Department of Psychiatry, University of Illinois, Chicago, Illinois
[3]Department of Computer Science, University of Illinois, Chicago, Illinois
[4]Division of Biostatistics, Department of Public Health Sciences, School of Medicine, University of California, Davis, California
[5]Department of Psychiatry and Behavioral Sciences, University of California, Davis, California
[6]Department of Psychology, Brigham Young University, Provo, Utah
[7]Pennington Biomedical Research Center, Louisiana State University, Baton Rouge, Louisiana
[8]Department of Neurology, University of California, Davis, California
[9]Department of Bioengineering, University of Illinois, Chicago, Illinois
[10]Department of Pediatrics, University of California, Davis, California

Abstract: Occurring in at least 1 in 3,000 live births, chromosome 22q11.2 deletion syndrome (22q11DS) produces a complex phenotype that includes a constellation of medical complications such as congenital cardiac defects, immune deficiency, velopharyngeal dysfunction, and characteristic facial dysmorphic features. There is also an increased incidence of psychiatric diagnosis, especially intellectual disability and ADHD in childhood, lifelong anxiety, and a strikingly high rate of schizophrenia spectrum disorders, which occur in around 30% of adults with 22q11DS. Using innovative computational connectomics, we studied how 22q11DS affects high-level network signatures of hierarchical modularity and its intrinsic geometry in 55 children with confirmed 22q11DS and 27 Typically Developing (TD) children. Results identified 3 subgroups within our 22q11DS sample using a K-means clustering approach based on several midline structural measures-of-interests. Each subgroup exhibited

Additional Supporting Information may be found in the online version of this article.

Contract grant sponsor: National Institute on Aging; Contract grant number: AG056782; Contract grant sponsor: National Institute of Mental Health; Contract grant sponsor: The Eunice Kennedy Shriver National Institute of Child Health and Human Development

*Correspondence to: Alex Leow; Departments of Psychiatry and Bioengineering, The University of Illinois at Chicago, 1601 W Taylor St, M/C 912, Chicago, IL 60612, USA. E-mail: aleow@psych.uic.edu and Tony J. Simon; Department of Psychiatry and Behavioral Sciences, University of California, Davis, CA, USA. E-mail: tjsimon@ucdavis.edu

Received for publication 5 December 2016; Revised 20 September 2017; Accepted 27 September 2017.

DOI: 10.1002/hbm.23838

Published online 00 Month 2017 in Wiley Online Library (wileyonlinelibrary.com).

distinct patterns of connectome abnormalities. Subtype 1, containing individuals with generally healthy-looking brains, exhibited no significant differences in either modularity or intrinsic geometry when compared with TD. By contrast, the more anomalous 22q11DS Subtypes 2 and 3 brains revealed significant modular differences in the right hemisphere, while Subtype 3 (the most anomalous anatomy) further exhibited significantly abnormal connectome intrinsic geometry in the form of left–right temporal disintegration. Taken together, our findings supported an overall picture of (a) anterior-posteriorly differential interlobar frontotemporal/frontoparietal dysconnectivity in Subtypes 2 and 3 and (b) differential intralobar dysconnectivity in Subtype 3. Our ongoing studies are focusing on whether these subtypes and their connnectome signatures might be valid biomarkers for predicting the degree of psychosis-proneness risk found in 22q11DS. *Hum Brain Mapp 00:000–000, 2017*.

Key words: 22q11DS; brain connectome; modularity; diffusion MRI; intrinsic geometry

INTRODUCTION

The chromosome 22q11.2 deletion syndrome (22q11DS), which also encompasses the phenotypes of velo-cardio-facial syndrome [Shprintzen et al., 1978] and DiGeorge syndrome [DiGeorge, 1965], is a neurogenetic syndrome due to a hemizygotic microdeletion at band 11.2 on the long arm of chromosome 22 [Edelmann et al., 1999; Shaikh et al., 2000; Shprintzen, 2000]. It likely occurs in more than 1 in 3,000 live births [Grati et al., 2015; McDonald-McGinn et al., 2015] and produces a complex and variable phenotype. Common manifestations include congenital heart defects, palatal and immunological anomalies, and craniofacial dysmorphisms and mild to moderate intellectual impairment [Shprintzen, 2008]. More specific cognitive impairments, which tend to be strongest in nonverbal domains, have recently been well characterized [Azuma et al., 2009; Bish et al., 2007; Campbell et al., 2010; McCabe et al., 2011; Shapiro et al., 2014; Van Aken et al., 2010; Wong et al., 2014]. A wide range of psychiatric diagnoses affect individuals with 22q11DS, with ADHD most common in childhood and anxiety seen at elevated levels (up to 60%) across the lifespan [Feinstein et al., 2002; Jolin et al., 2012]. These disorders, particularly anxiety, can be substantially impairing on everyday function [Angkustsiri et al., 2012] and increasing the already high risk for schizophrenia [Gothelf et al., 2013; Tang et al., 2014], which, strikingly affect 25%–30% of adults [Green et al., 2009; Murphy et al., 1999; Schneider et al., 2014]. This makes 22q11DS the strongest genetic risk factor for such outcomes [Karayiorgou et al., 2010] aside from having a monozygotic twin or two affected parents with the disorder [McGuffin et al., 1995]. Also, very common across the lifespan are social functioning impairments in various forms, leading to frequent but possibly inappropriate diagnoses of autism spectrum disorder [Angkustsiri et al., 2014; Eliez, 2007; Vorstman et al., 2006].

Structural neuroimaging studies of children with 22q11DS have reported volumetric brain abnormalities, including reductions in total brain volume [Tan et al., 2009], but particularly in white matter volume [Eliez et al., 2000; Kates et al., 2001], and gray matter in the left parietal lobe [Eliez et al., 2000]. In addition, midline anomalies in brain structures, many loosely associated with schizophrenia, have been reported frequently in 22q11DS. These include dilated ventricles, anomalous corpus callosum, small hippocampi, and altered fornix integrity [Campbell et al., 2006; Deng et al., 2015; Debbane et al., 2006; Kates et al., 2015; Machado et al., 2007; Shashi et al., 2012; Simon et al., 2005c]. Several studies have reported an increase in the size of the cavum septum pellucidum and cavum vergae (CSP/CV) in 22q11DS [Beaton et al., 2010; Campbell et al., 2006; Schmitt et al., 2014; Shashi et al., 2004]. An enlarged CSP has also been associated with schizophrenia [Galarza et al., 2004]. In the largest sample to date of children with 22q11DS, Beaton et al. [2010] found that children with 22q11DS were more likely to have *Abnormal* CSP/CVs, defined as an anteroposterior length of 7–10 mm [Nopoulos et al., 2000], than typically developing (TD) children. Beaton et al. [2010] additionally found greater CSP/CV volumes that had previously been reported in the literature, and thus proposed an *Extreme* group of an anteroposterior length of 12 mm or greater. They found that only individuals with 22q11DS were classified in this Extreme group. Despite the fact that all the above midline anomalies have been associated with the incidence of schizophrenia [Shenton et al., 2001], the relationships between these anomalies in those with 22q11DS at risk for, or already found to have schizophrenia, have not been extensively investigated to date. Given how frequently these anomalies occur in children with 22q11DS and given how variable the neural, and other, subphenotypes can be, we wanted to use a completely data-driven approach to determining if that variability might actually contain identifiable subtypes based on measures of these schizophrenia-relevant structures. If such subtypes did exist, researchers could determine factors such as differential patterns of connectivity and/or relationships to the spectrum of schizophrenia symptoms in adolescents and young adults. Should any such relationships exist, then

the subtypes could be used as predictive biomarkers for differential developmental patterns in young children that could prove powerful for early identification and intervention for individuals at highest risk of developing psychosis.

Recently, attention has turned to analyzing the differences in structural and functional connectivity that may be associated with these neuroanatomical anomalies. Alterations in resting state connectivity have been reported in 22q11DS [Scariati et al., 2014]. For example, using connectomics, Ottet et al. [2013] found a global degree reduction of 6% in the networks of patients with 22q11DS, and a decrease of global efficiency in patients with 22q11DS compared to healthy controls. They found that 58% of hubs were reduced in 22q11DS, including the left thalamus, bilateral hippocampal, parietal, and precentral regions. Furthermore, a negative correlation was found between schizophrenia spectrum symptom severity and local efficiency in Broca's and Wernicke's areas, contrasting with a positive correlation with the dorsolateral prefrontal cortex (DLPFC). In a more recent study with a partly overlapping sample, Váša et al. [2016], using a weighted graph theoretical analysis, identified the spatial distribution of the regions driving the global network integration deficit in 22q11DS. They termed this subset of regions the "affected core" of the 22q11DS structural connectome. This subnetwork of the connectome, which contains regions that are particularly important for efficient network communication, was less densely connected in 22q11DS. The affected core consisted of numerous nodes, many of which were network hubs, which were mostly bilaterally symmetric and located in the frontal and parietal cortical regions, and subcortical structures including the thalamus and hippocampus. They also observed that the mean connectivity strength and efficiency in the orbitofrontal-cingulate circuit correlated negatively with extent of negative symptoms in patients with 22q11DS.

Though several studies have now adopted connectomics to investigate structural connectivity in 22q11DS, none to our knowledge has utilized advanced computational connectomics techniques to investigate higher level connectome properties of modularity (i.e., the community structure of networks). Thus, in this study, we sought to use a recently developed, innovative technique for investigating the hierarchical modularity of brain networks known as PLACE, or Path Length Associated Community Estimation [GadElkarim et al., 2012, 2014]. General analyses were carried out by comparing brain image data from 55 children with 22q11DS to those from 27 typically developing (TD) children. However, of much greater interest was whether patterns of neural connectivity are different *within* the sample of children with 22q11DS. Therefore, we also investigated the hypothesis that patterns of connectivity would be more anomalous in the cluster that contained the most atypical brains of children with 22q11DS in our sample than in the cluster that contained the least atypical brains of children with 22q11DS in our sample. To test this hypothesis, we examined whether the brain's hierarchical modularity in children from each of three 22q11DS subgroups that we had identified (see below) differed significantly from the pattern seen in the brains of typically developing children and if any patterns of connectivity were associated with behavioral phenotypes.

METHODS

Participants

A total of 82 children, including 55 diagnosed with 22q11DS (mean age = 11.22± 2.58 years, 25 males) and 27 typically developing (TD) (mean age = 10.61 ± 2.4 years, 14 males), participated in this study conducted in the MIND Institute's 22q11.2 Research Center and Clinic, University of California Davis. Behavioral symptoms were frequent in individuals with 22q11.2DS, with elevated scores for 51% of participants on measures of childhood anxiety (Behavior Assessment for Children and Spence's Anxiety Scale) [Reynolds and Kamphaus, 2004; Spence, 1999], 33% for ADHD (The SNAP-IV Rating Scale) [Swanson et al., 1992], and 20% with social communication impairments (Social Communication Questionnaire) [Rutter et al., 2003]. Written informed consent was obtained from all participants and their guardians. Diagnosis of chromosome 22q11.2 deletion was confirmed using fluorescent in situ hybridization (FISH) or a similar genetic test. Parents provided all genetic test data as part of the screening process. All protocols were approved by the Institutional Review Board of University of California Davis Medical Center.

MRI Acquisition

Participants were scanned at the Imaging Research Center at the University of California at Davis Medical Center on a 3 T Siemens MAGNETOM Trio scanner with a Tim operating system. A 32-channel head coil was used to acquire T1-weighted and diffusion-weighted MRI. The 3D magnetization-prepared rapid gradient-echo (MPRAGE) T1-weighted sequence with isotropic voxel dimension parameters were as follows: sagittal plane of acquisition, 192 slices, slice thickness 0.9 mm, number of excitations = 1, repetition time (TR) 2,200 ms, echo time (TE) 4.37 ms, inversion time 1,100 ms, flip angle 7°, field of view 230 × 230 mm, matrix 256 × 256, bandwidth 260 Hz/voxel. For diffusion-weighted MRI data, 64 contiguous axial brain slices were collected with the following parameters: 60 diffusion-weighted ($b = 700$ s/mm^2) and 2 ($b = 0$ s/mm^2) non-diffusion-weighted scans, field of view 280 mm, voxel size 0.9 × 0.9 × 1.8 mm, TR = 20 ms, TE = 5 ms.

Structural Network Reconstruction

Initially, 82 regions of interest (ROIs) were defined on each participant's T1 MRI using a standard Freesurfer (v5.3; http://surfer.nmr.mgh.harvard.edu/) parcellation

pipeline (recon-all option) and the Desikan atlas [Desikan et al., 2006]. Diffusion-weighted MRI was preprocessed using FSL (http://fsl.fmrib.ox.ac.uk/fsl) including scalp removal with the *bet* function [Smith, 2002] and correction for eddy current distortion using the *eddy_correct* function [Andersson and Sotiropoulos, 2016]. The gradient table was adjusted accordingly. After preprocessing, we performed whole-brain tractography using Fast Assignment Continuous Tracking (FACT) algorithm [Mori et al., 1999]. Fiber tracking was restricted among voxels with fractional anisotropy (FA) values higher than 0.2, which indicate typical white-matter regions. The fiber-tracking critical angle was set to 35° based on the data quality and our prior experience. To account for field inhomogeneities, each participant's FA image was nonlinearly registered to the corresponding T1 MRI space using the *Symmetric Normalization* (Syn) method [Avants et al., 2008] in Advanced Normalization Tools (ANTs) [Klein et al., 2009] package and the resulting deformation field was then applied to the tractography. An 82 × 82 brain network was then reconstructed for each participant by counting the ratio of total number of fiber streamlines connecting each pair of ROIs [Zhan et al., 2015]. Each value in the matrix indicates the connection strength (or connectivity) between two corresponding ROIs.

Definition of 22q11DS Subtypes

As part of an ongoing research project seeking to identify neural biomarkers of outcomes in youth with 22q11DS, one of our labs (TJS) has been exploring whether any inter-relationships exist between several frequently reported anomalies in or near the midline of brains of individuals with 22q11DS [Simon et al., 2016]. These structural anomalies are not only robust features of the 22q11DS phenotype but also the same structures that are repeatedly reported to be anomalous in the brains of people with schizophrenia [Shenton et al., 2001]. Therefore, given the extremely high risk for schizophrenia in people with 22q11DS, we wanted to determine (a) if there were detectable subtypes and (b) if we could later relate this to schizophrenia symptoms when the children in this study were re-enrolled and evaluated in late adolescence. Thus, we entered values computed from T1-weighted structural and diffusion-weighted MR brain images of the 55 children with 22q11DS in this study into a K-means clustering analysis to see if there were separable clusters within which these values systematically varied. Entered values were volumes of left and right hippocampus [Scott et al., 2016], lateral ventricles, five subsections of the corpus callosum, and the cava (CSP/CV). Also entered was the length (in millimeters) of the cava [Beaton et al., 2010] and the average fractional anisotropy (FA) and radial diffusivity (RD) of the fornix [Deng et al., 2015]. Based on this analysis, we identified three subtypes of 22q11DS, described in the Results section. Please refer to Supporting Information, Figure 3 for the scree plot for our K-means clustering analysis, which guided us to select three as the number of clusters.

Statistical Analysis

Initial analyses use a generalized linear regression to evaluate the effect of age, sex, and subject type (TD or 22q11DS Subtype 1, 2, and 3) on several standard network measures [Rubinov and Sporns, 2010] including global and nodal efficiency, characteristic path length, clustering coefficient, and small-worldness. We found that neither age nor sex had any significant effect on all network measures (for effect sizes and the corresponding P values please refer to Supporting Information, Table 1). Thus, in the following modularity analysis, age and sex were not entered as co-varying variables.

Modularity Analysis

Using PLACE (Fig. 1A) [GadElkarim et al., 2012, 2014], we investigated differences between 22q11DS and TD using a hierarchical permutation approach, illustrated in Figure 1B.

Owing to the hierarchical nature of PLACE trees, controlling for multiple comparisons is straightforward. Indeed, using permutation analyses, if a region exhibits different nodal affiliations between 2 groups at each of the highest m levels of modular hierarchy (each of them controlled at 0.05), collectively all m levels would yield a combined false positive rate of 0.05^m. Since PLACE trees are computed using 82 × 82 structural connectomes up to level 4 (yielding $2^4 = 16$ communities), significant nodal affiliation differences are thus defined as any region that exhibits significant nodal affiliation differences with permutation testing (at $P = 0.05$) for levels 2, 3, and 4 (as 0.05^3 is $<0.05/82$, thus surviving the more stringent Bonferroni correction).

Intrinsic Geometry Analysis

We also used PLACE to examine a related and novel concept of connectome's intrinsic geometry in 22q11DS using the *BRAINtrinsic* approach [Conte et al., 2015]. This approach is especially useful for visually understanding connectomes in an intuitive way, and is akin to the visualizations that cartographers use to map quantitative data onto world maps. In such maps, information is displayed relatively, such as when countries are resized on a map according to their gross domestic product (GDP). When this is done, it becomes obvious that the U.S. has the largest GDP. The BRAINtrinsic approach intuitively determines the coordinates of each brain region using the interconnectivity that each region has with the rest of the brain, independent of its anatomical location. Thus, rather than displaying physical proximity, in the three-dimensional graphs produced by this approach, ROIs that are displayed closer together are those that have stronger

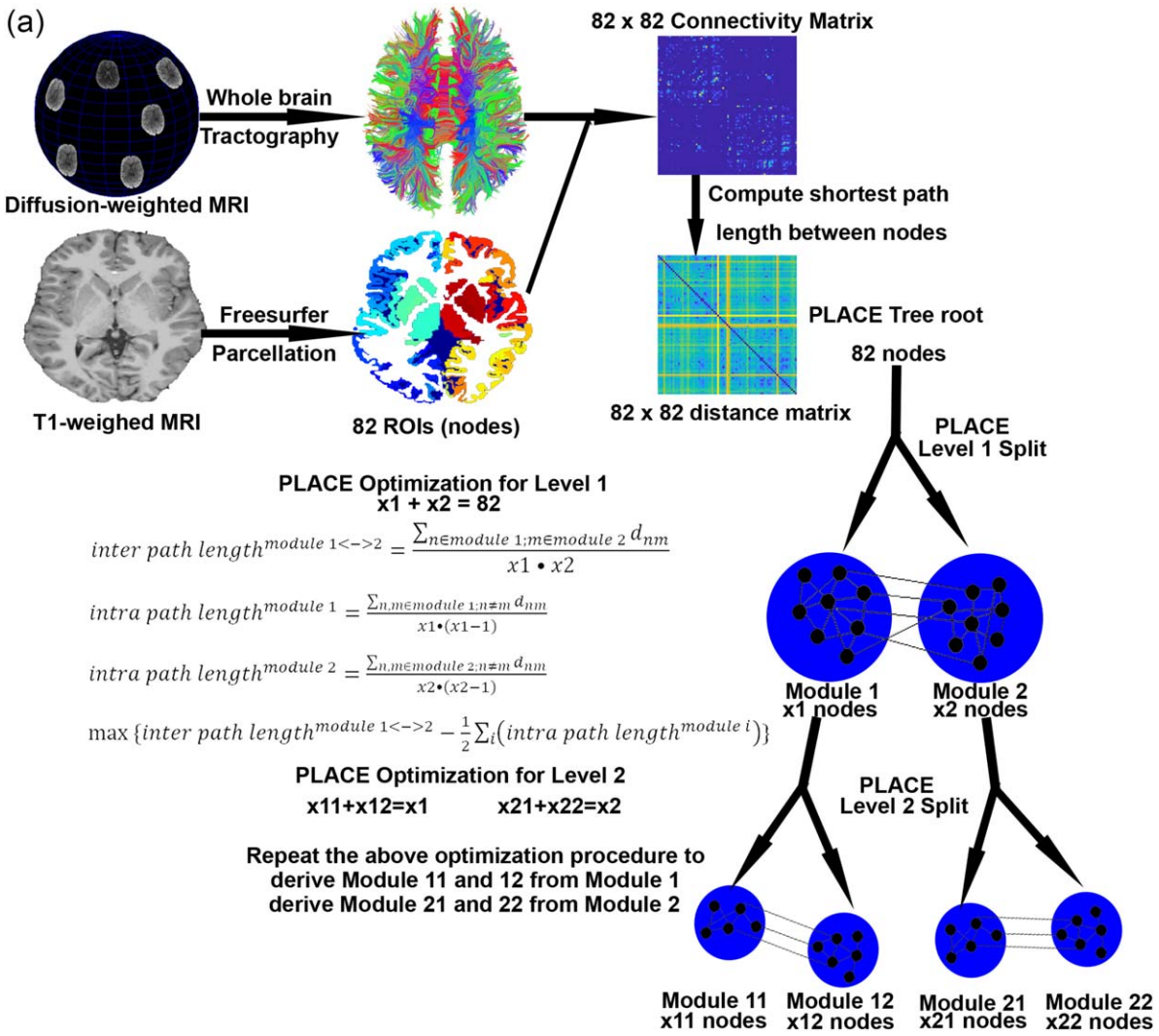

Figure 1.

(A) Illustration of PLACE algorithm. Please refer to GadElkarim et al. [2012, 2014] for more detail. (B) Illustration of PLACE hierarchical permutation procedure. [Color figure can be viewed at wileyonlinelibrary.com]

connections between one another than ROIs that are displayed further apart.

To understand a connectome's intrinsic geometry, high-resolution connectivity matrices are needed. We used our previously published upsampling approach [Ye et al., 2015] to further subdivide each Freesurfer ROI until all of its components reached a size of ~2,000 voxels, yielding upsampled connectivity matrices of size 572 × 572. To account for potential scaling confounds secondary to variable total fiber counts, we normalized each subject's upsampled connectivity matrix to have unit mass, that is, the matrix is normalized by the total fiber count for that subject, such that every subject contributes equally to the group geometry. Then we computed the mean matrix of each group by averaging across all normalized individual matrices for that group followed by the extraction of both group-level and individual-level connectome's intrinsic geometry using isomap embedding of the corresponding pairwise shortest graph distance matrix. We compared group intrinsic geometry measures for each of the 22q11DS clusters to the TD group's values in order to determine if any of the 22q11DS clusters differed significantly from the pattern seen in typical development.

Functional Correlate Analysis

Given the 7–14 years old age range of the participants reported in this article (our study Phase I or baseline

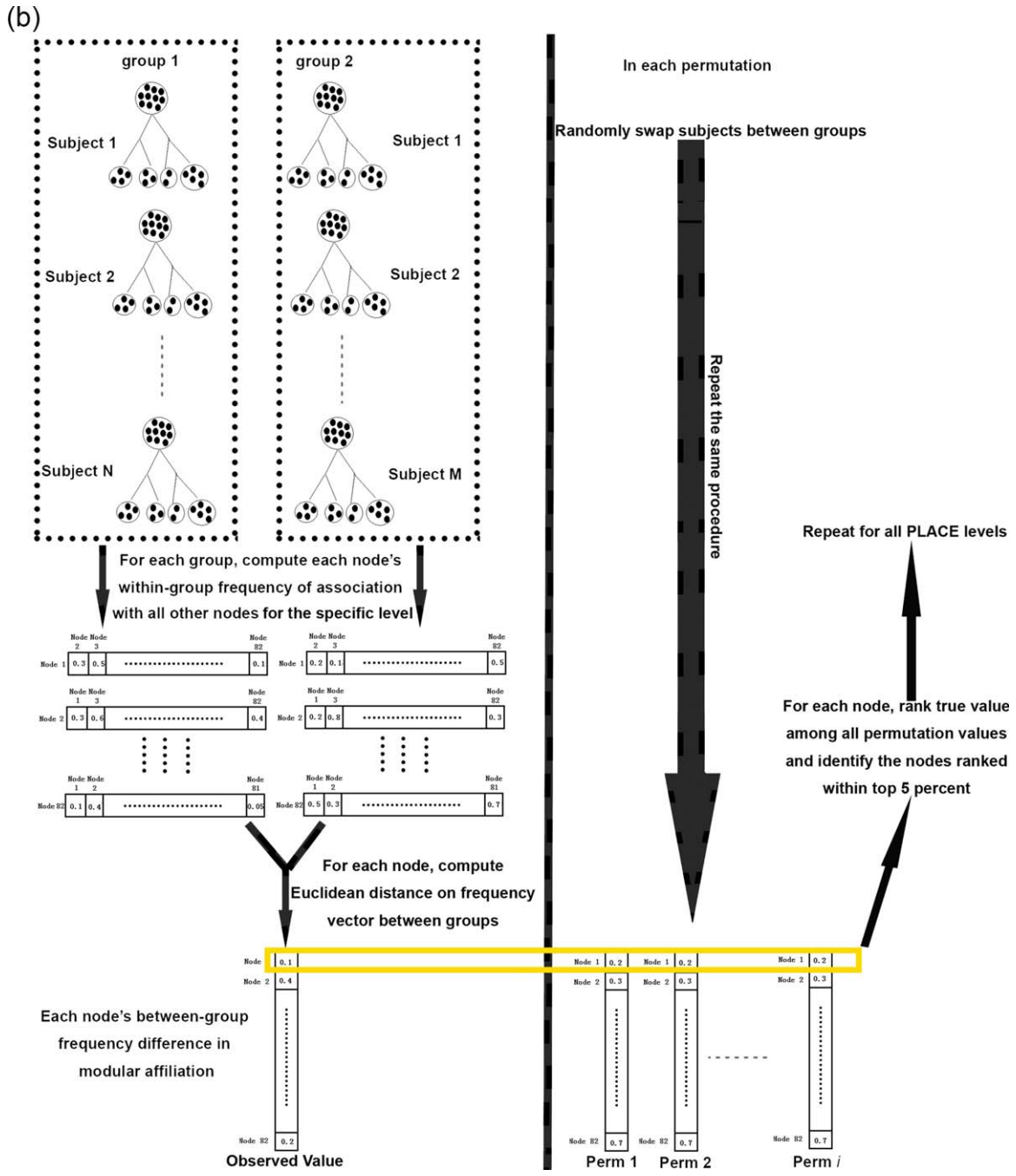

Figure 1.
Continued.

assessment), it was not possible to assess one of the two main 22q11DS subphenotypes of interest in our research, namely psychosis spectrum symptomology. This was due to two factors. One is the rarity of such symptoms before late adolescence. The other is that exaggerated conceptual weakness due to cognitive impairment makes it very difficult to reliably complete a structured interview involving complex, abstract questions about unusual thought experiences. Those interviews are currently being conducted with most of the Phase I participants who are participating in our study Phase II, a longitudinal assessment of cognitive and affective functions and their relationships to psychosis proneness symptoms in youth aged 12–18 years of age who will return for further assessment at 15–21 years

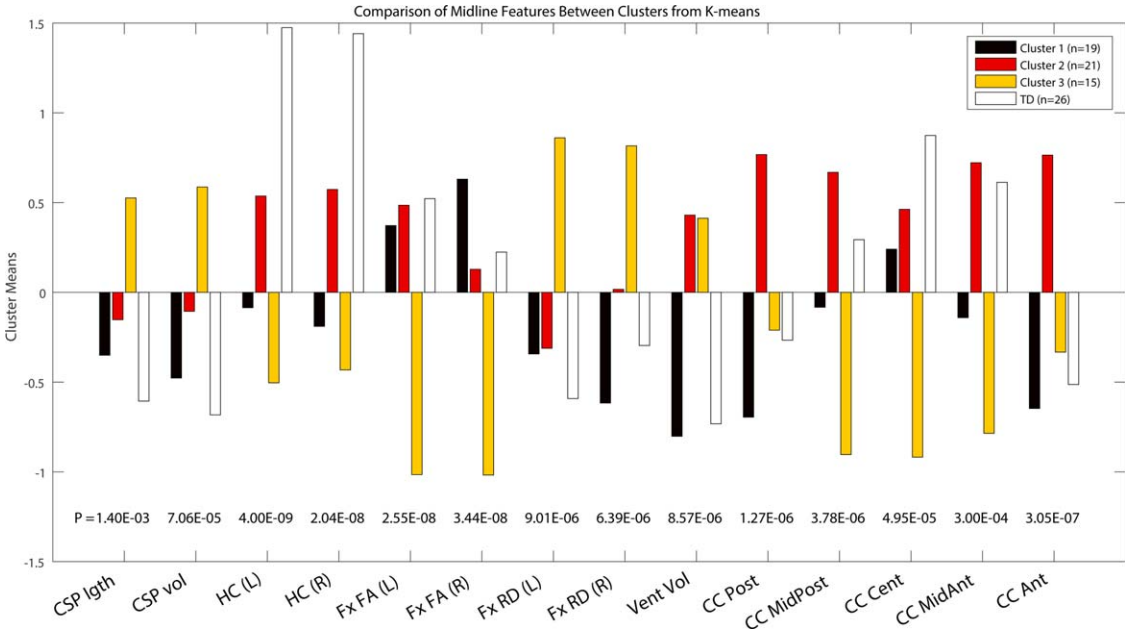

Figure 2.

Result of the K-means clustering analyses. *Y*-axis values are Cluster means *Z* scores zeroed at the average value for the entire 22q11DS group ($N = 55$). *P* values are computed from the one-way ANOVA for these four groups in each of 14 measures. [Color figure can be viewed at wileyonlinelibrary.com]

old. We did have measures of the more common childhood behavioral disturbances such as anxiety, ADHD, and social impairment symptoms. These were collected using the Spence Childhood Assessment Scale [Spence, 1999], SNAP-IV ADHD scale [Swanson et al., 1992], and the Social Competence Questionnaire [Rutter et al., 2003]. We also collected data on a number of information processing experimental paradigms developed in our laboratory to measure degree of impairment, relative to typically developing age-matched peers, in spatial and temporal visual and auditory information processing. Linear regression or repeated measures regression models were used to assess the association between network measures and childhood behavioral disturbances or information processing in children with 22q11DS. All models covaried age and sex, and assumptions of the models were checked and met by the data.

RESULTS

K-Means Clustering Analysis

Scree plots resulting from the analysis indicated that a 3-cluster (subtype) model was the most effective without resulting in cluster sizes that were too small, accounting for 32% of the variance. Because we were interested in the relationship between anomalous structures within the brains of children with 22q11DS, values from TD controls were not entered into this analysis but were compared with subtype values subsequently. Subtype 1 ($n = 19$) contained generally healthy-looking brains with values most similar to those of the TD group for every value except left and right hippocampal volumes, which were around 1.5 SD smaller in this 22q11DS subgroup. Subtype 2 ($n = 21$) contained brains that had an array of atypical values. Hippocampal volumes in this cluster were the closest of all subtypes to the TD values (1.0 SD smaller) and fornix scalar values tracked the TD values closely. However, cava volumes and lengths were almost 0.5 SD larger, and lateral ventricle volumes were 1.0 SD larger than in the TD group. Finally, the two most posterior and one most anterior callosal section volumes in this group were 0.25–0.75 SD larger than those of the TD group even though the three central sections matched the TD group's almost identically. Subtype 3 ($n = 15$) contained grossly anomalous brains, easily visible as such to the naked eye. Cava values were 1.0 SD larger and hippocampal volumes were 2.0 SD smaller than the TD group's. Fornix scalar values had the opposite pattern to the TD group's, with RD values being 1.0 SD higher and FA values being 1.0 SD lower. Ventricle volumes, like Subtype 2, were 1.0 SD larger than in the TD group. In direct contrast to Subtype 2, Subtype 3's most posterior and anterior corpus callosum segment volumes were identical to the TD group but all the others were 0.75–2.0 SD smaller. The results of the k-means clustering analysis are presented in Figure 2, with exemplary brain images from each Subtype depicted in Figure 3A. To confirm the findings of the k-means

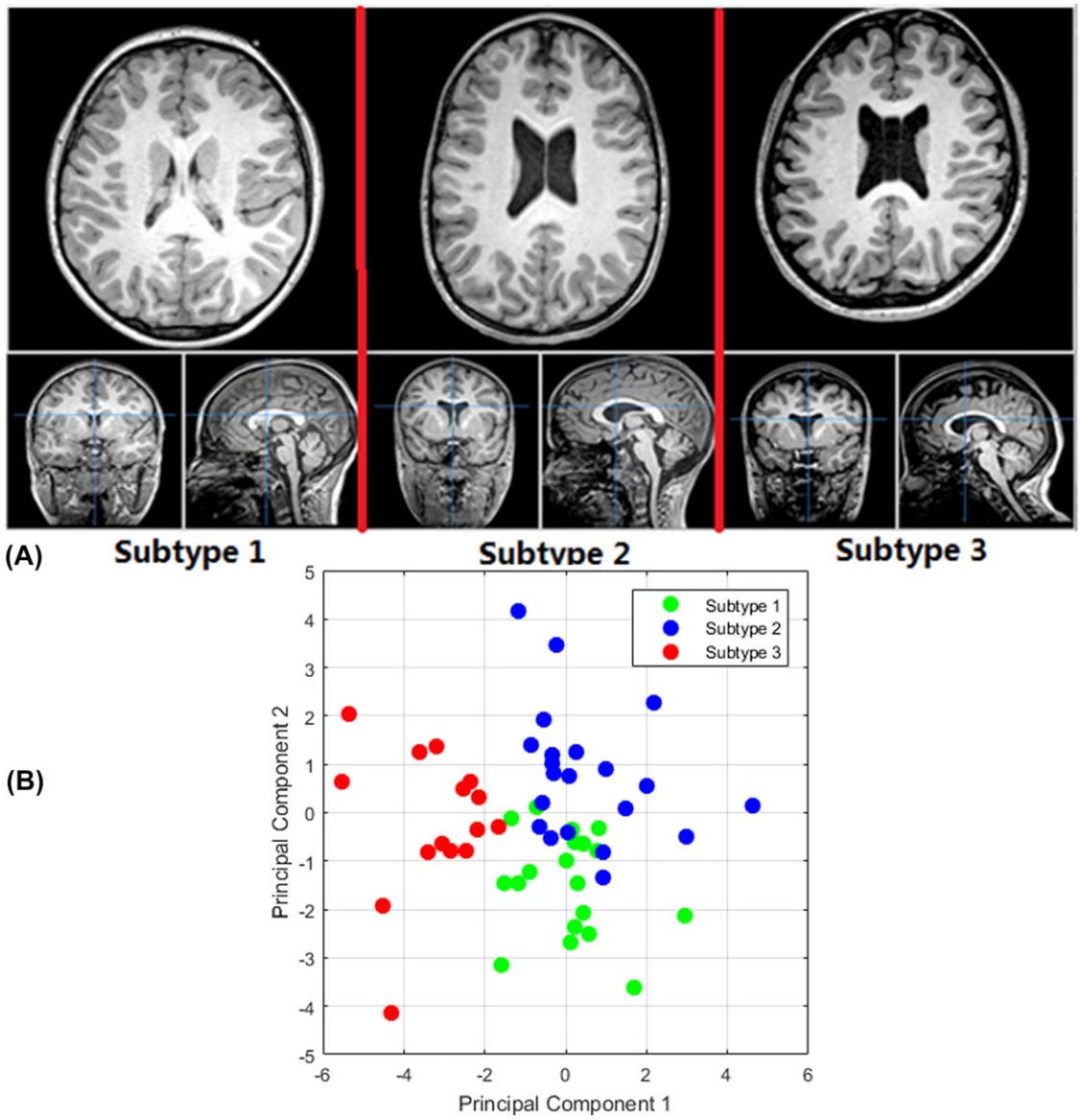

Figure 3.

(A) Exemplary brain images from each cluster subtype. (B) Principal component analysis (PCA) for the 14 measures depicted in Figure 2, with the first two principal components showing a visually obvious clustering pattern for three subtypes. [Color figure can be viewed at wileyonlinelibrary.com]

clustering with an independent method, we carried out principal components analysis (PCA) on these 14 measures. This confirmed the findings of the clustering analysis as is clearly depicted in Figure 3B.

PLACE Hierarchical Modularity Analysis

We conducted permutation-based hierarchical modularity analysis using the PLACE-derived hierarchical binary trees. Comparison of each 22q11DS subtype to TD revealed significant hierarchical modular differences: (a) between Subtype 2 and TD in the right hippocampus and the right precentral gyrus; (b) between Subtype 3 and TD in the right pars orbitalis, pars triangularis, posterior cingulate, and precuneus. By contrast, no significant differences were detected between Subtype 1 and TD.

Figure 4 (Panel A) shows that the right hippocampus was more associated with parietal regions in the TD group than in 22q11DS Subtype 2, including the bilateral precuneus and isthmus of the cingulate, and the left posterior

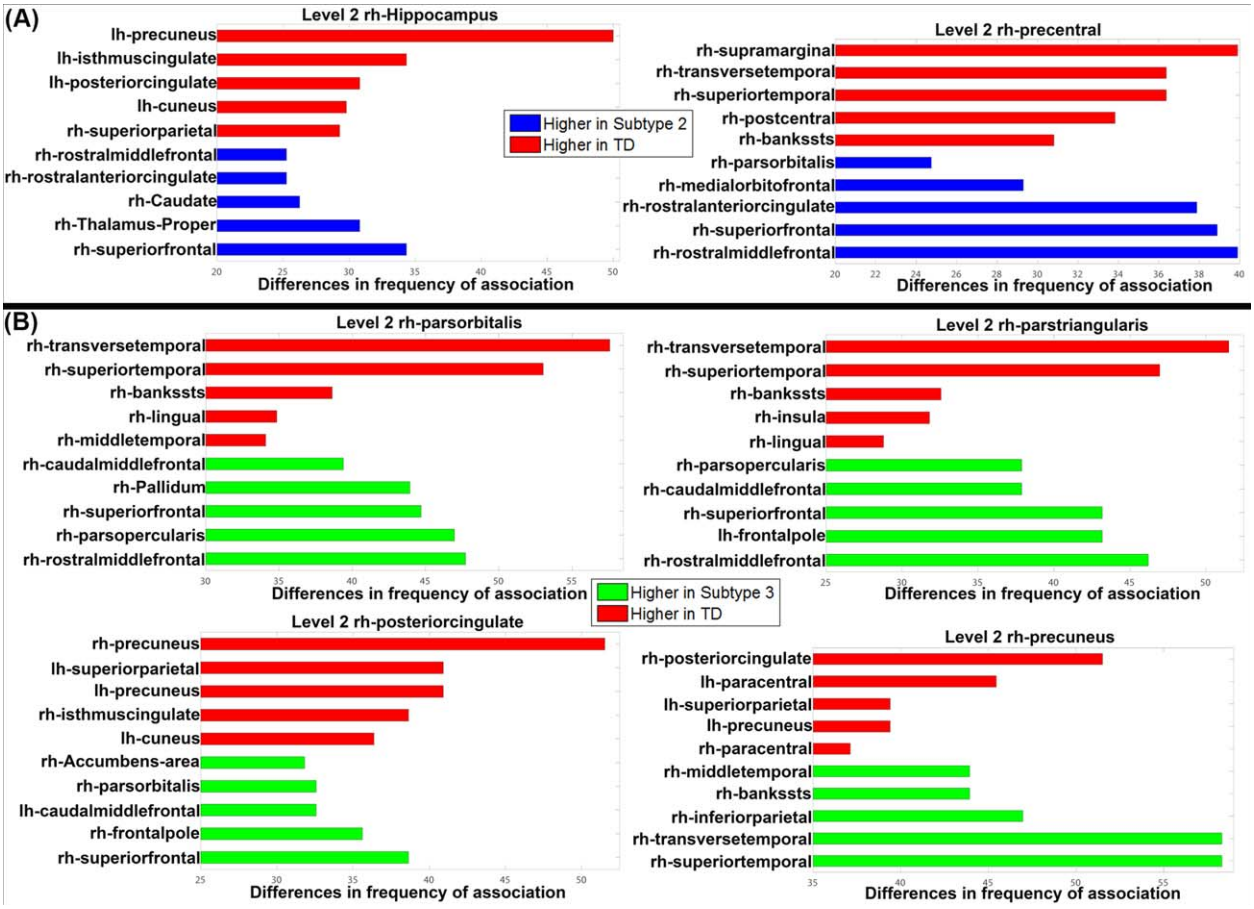

Figure 4.

Frequency bar graphs showing the top 5 differences in the frequency of association, between other regions (*y*-axis) and the region-of-interest (top), for TD and 22q Subtypes 2 (panel A) and 3 (panel B), arranged by the magnitude and direction of differences. Red bars indicate more frequent associations in TD while blue bars indicate more frequent associations in 22q Subtype 2 and green bars more frequent associations in Subtype 3 (please refer to Supporting Information, Fig. 1A–F for more detail). [Color figure can be viewed at wileyonlinelibrary.com]

cingulate cortex and right superior parietal lobule. In the opposite direction, the right hippocampus was more associated with the right hemispheric frontal regions, including the superior frontal gyrus, rostral middle frontal gyrus, anterior cingulate cortex, caudate, and the thalamus in Subtype 2 compared to the TD group.

Subtype 2 also differed from the TD group in an ROI located in the right precentral gyrus. This was more associated with right hemisphere parietal and temporal regions in the TD group than Subtype 2, including the supramarginal, transverse, and superior temporal gyri. For Subtype 2, the precentral gyrus was more associated with other frontal regions, including rostral middle frontal, superior frontal, and rostral anterior cingulate cortex.

The second set of significant findings to emerge from the PLACE analyses concerned Subtype 3 in relation to the TD group (Fig. 4, Panel B). First, both the right pars orbitalis and the pars triangularis ROIs were more associated with right hemisphere temporal regions in the TD group than in Subtype 3, including in the transverse and superior temporal gyri and the bank of the superior temporal sulcus. In the opposite direction, both the right pars orbitalis and the pars triangularis ROIs were more associated with right hemisphere frontal regions in Subtype 3 compared to the TD group, including the rostral middle frontal and superior frontal gyri, and the pars opercularis, and parts of the basal ganglia, including the caudate.

Figure 5 shows the 3D cortical surface plots (of nodal affiliations) comparing TD with Subtype 2 (Panel a) and Subtype 3 (Panel b). Warm colors identify regions more likely to be assigned to the same local community as the labeled ROI in the TD group. Cold colors identify regions

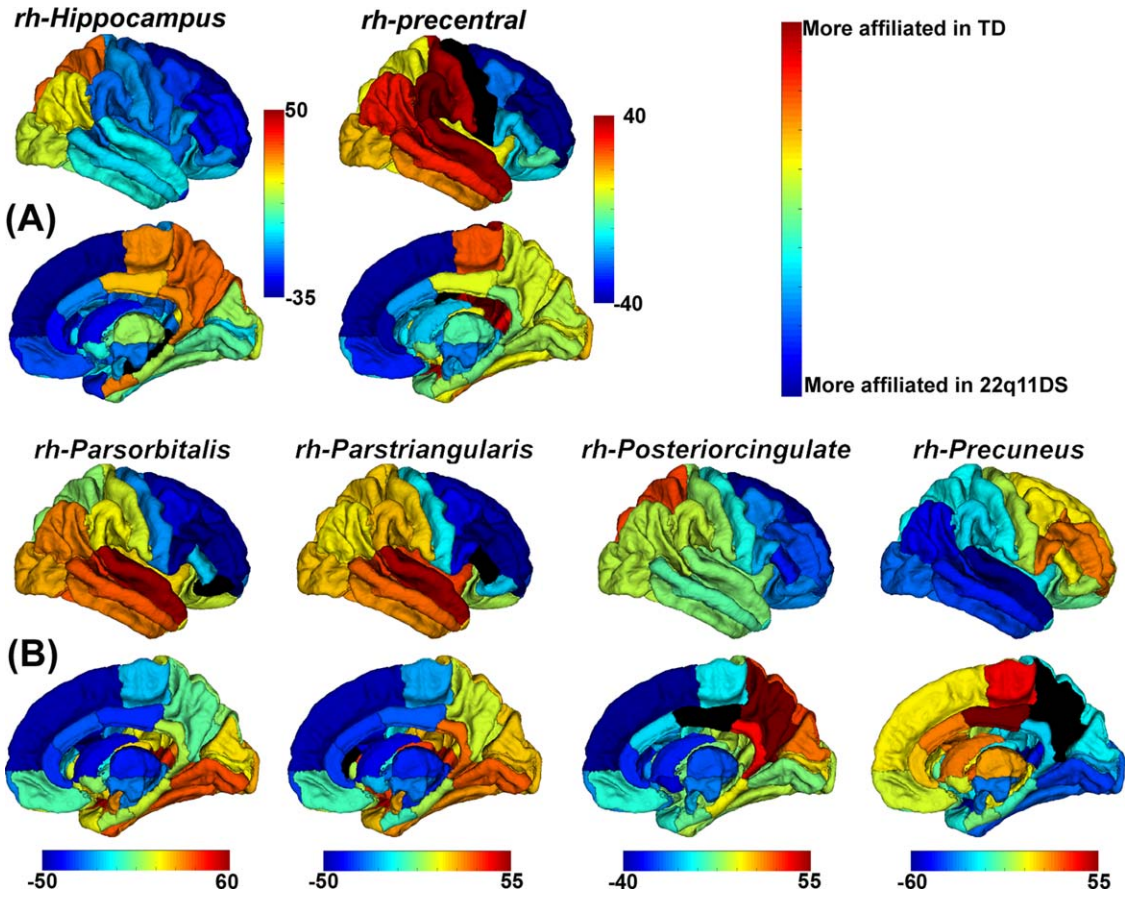

Figure 5.

Three-dimensional surface plots (of nodal affiliations) showing differences (in %) between TD and 22q11DS Subtype 2 (Panel a) and Subtype 3 (Panel b). Warmer colors indicate that a region is more affiliated with the region-of-interest (black) in TD group compared with 22q11DS Subtype 2 (Panel a) or 3 (Panel b); cooler colors represent the opposite. [Color figure can be viewed at wileyonlinelibrary.com]

more likely to be assigned to the same local community as the labeled ROI in the 22q11DS Subtypes.

Global Intrinsic Geometry Analysis

Visual inspections of group-level mean intrinsic geometries (Supporting Information, Fig. 2) suggested that there is a relative disintegration in 22q11DS Subtype 3 relative to the TD group in temporal-occipital regions. This finding was supported by statistically comparing individual-level lobar integration, measured using the Hausdorff point cloud distances [Taha and Hanbury, 2015] between lobar positions in the left and right hemisphere in their isomap embeddings, for each 22q11DS Subtype relative to the TD group. Two-sample t tests confirmed that temporal lobe integration was significantly greater (i.e., a larger Hausdorff distance) in 22q11DS Subtype 3 relative to the TD group ($P = 0.0062$, statistically significant with a Bonferroni correction of $P = 0.05/3$; Fig. 6), suggesting very atypical intertemporal connectivity in this 22q11DS Subtype that had the most anomalous brains.

Overall, the results from PLACE and intrinsic geometry analyses suggest an abnormal, differentially altered connectivity profile anterior-posteriorly in our total 22q11DS sample. In particular, Subtypes 2 and 3 do not show the same pattern of fronto-parietal/fronto-temporal connectivity that is evident in the TD group. Furthermore, Subtype 3 demonstrates greater precuneus to temporal lobe but reduced inferior frontal gyrus to temporal lobe connectivity than the TD group, in addition to reduced hemispheric integration of the temporal lobes.

Functional Correlates

Analysis of variance (ANOVA) of IQ, and the cognitive and behavioral measures collected on this school-aged sample of children with 22q11DS revealed no differences

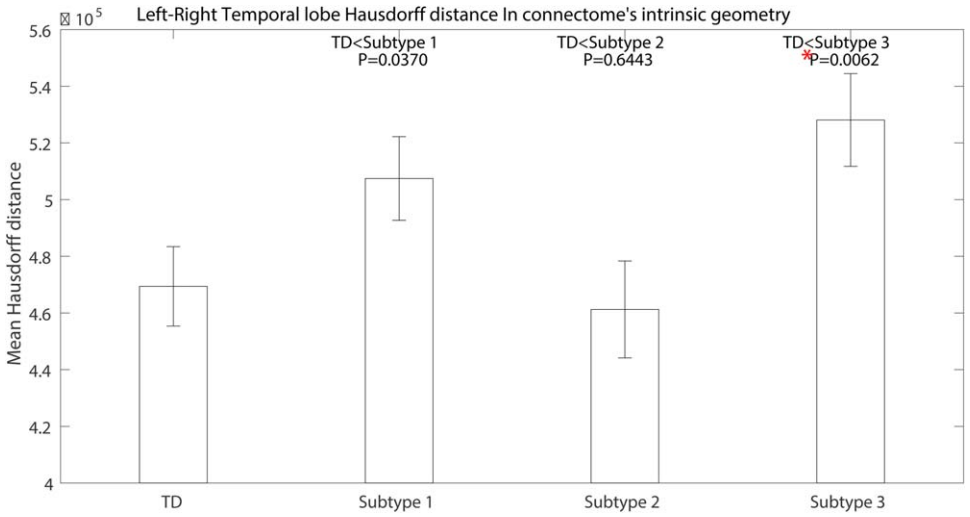

Figure 6.
Group differences in Hausdorff point cloud distances between left and right temporal lobar positions. [Color figure can be viewed at wileyonlinelibrary.com]

between the 3 brain subtype groups even though the general population of children with 22q11DS is consistently found to be different from their typically developing peers on these or similar measures. As discussed later, none of these measures was directly related to schizophrenia risk, so this result was not entirely unexpected. We do expect to find differences in our future studies that compare schizophrenia symptoms within these brain subtype groups.

Despite the high rate of elevated symptoms in all the anxiety, ADHD, and social impairment measures, no relationships were found with measures of intrinsic geometry. Also, despite the significant group differences demonstrating impairment in the 22q11DS group relative to TD peers in all of the spatial and temporal cognitive processing tasks we deployed, no relationships were found between functional abilities and measures of brain connectivity.

DISCUSSION

Using state-of-the-art computational connectomics, this study conducted two main complementary analyses to compare patterns of connectivity in subgroups of a sample of 55 children with 22q11DS with that seen in 27 typically developing children. We used a data-driven approach to determine whether neural subtypes existed within our sample using measures of schizophrenia-relevant structures. As stated in Results, we identified three clusters based on a combination of a scree plot and the resulting cluster sizes (to ensure that we were not running analyses on clusters that were too small). In fact, the 4-cluster solution resulted in clusters of size 16, 8, 18, and 13 (rather than the 19, 21, and 15 of the 3-cluster solution). We decided on the 3-cluster solution to have sufficient information in each of the clusters to provide meaningful comparisons. Our motivation was to determine whether such subtypes could be identified because tools to reduce the phenotypic variability in 22q11DS could be extremely powerful. If the future research is able to replicate such subtypes in other samples and use them to identify patterns, detectable in early childhood, that might predict risk for or protection against schizophrenia symptoms or full-blown psychosis in late adolescence or early adulthood, then the research contribution would be some extremely powerful biomarkers for later outcomes.

The PLACE analysis of hierarchical modularity revealed significant differences between the TD group and 22q11DS Subtypes 2 and 3 but only in the right hemisphere. The right hippocampus was more affiliated with frontal regions in 22q11DS Subtype 2, but more affiliated with occipital and parietal regions in the TD group. Similarly, the precentral gyrus was also more affiliated with frontal regions in 22q11DS Subtype 2 compared to a stronger affiliation with temporal and inferior parietal regions in the TD group. For 22q11DS Subtype 3, the right pars orbitalis and pars triangularis showed a similar pattern in which they were more affiliated with frontal regions but in the TD group these two frontal opercular regions were more affiliated with temporal regions. The posterior cingulate cortex (PCC) affiliation in 22q11DS Subtype 3 was strongest with frontal regions, while in the TD group, it was strongest with superior parietal regions. Finally, the precuneus in Subtype 3 was most strongly affiliated with occipital and temporal regions in contrast to the strongest affiliation with medial central regions in the TD group.

The global intrinsic geometry analysis carried out with BRAINtrinsic revealed a relative disintegration of temporal-occipital regions in 22q11DS Subtype 3 (i.e., those

with the most grossly anomalous medial brain structures) relative to the TD group. Computation of Hausdorff distances between lobar positions in the left and right hemispheres revealed a statistically significant difference for the temporal lobes in Subtype 3 relative to the TD group. This suggests that a very atypical pattern of connectivity between the left and right temporal lobes exists in these children with 22q11DS. Without further investigation, it is not possible to understand the relationship of this pattern to the significantly different values of the brain regions that separate those in Subtype 3 from the other group. Nor is it clear what the functional implications of this are, as there were no correlations between any subtype with ADHD, anxiety, or social communication impairments, nor between these distance values and performance on a range of cognitive tasks that the same children completed. However, those tasks were not designed as tests of temporal lobe connectivity. Also, because of the young age and intellectual impairment of the children with 22q11DS, we did not attempt to assess psychotic thinking symptomology in this group. Therefore, we must conclude that the connective differences that we report appear not to be related in any obvious way to the behavioral or spatial and temporal information processing impairments that are so characteristic of children with 22q11DS. This does not mean, of course, that the same will be true of perhaps the most clinically and functionally significant outcome for a strikingly large minority of people with 22q11DS, that of schizophrenia spectrum disorders and the associated intermediate phenotype of impaired executive function. Many of the Phase I participants reported on here are being followed longitudinally with those measures, and so we will be carrying out our first analyses of these relationships in the not too distant future.

Neither of our analytical approaches revealed significant differences between the TD group and Subtype 1. Together with our finding the most significant differences between Subtype 3 and the TD group, this supports our hypothesis that patterns of connectivity should be more anomalous in the cluster that contained the most atypical brains of children with 22q11DS in our sample than in the cluster containing the least atypical brains of children with 22q11DS.

The level 2 PLACE hierarchical modularity differences for Subtype 2 indicate very unusual patterns of nodal affiliation, further indicating distinct connectivity patterns relative to the TD group or the least anomalous brains of 22q11DS Subtype 1. The prominence of the right hippocampus in these findings is important because hippocampal volume reduction has been repeatedly found in 22q11DS [Debbane et al., 2006], and appears to be associated with lower Full Scale, Verbal, and Nonverbal IQ scores [DeBoer et al., 2007]. Specific regional volume reductions within the left and right hippocampi have also been associated with the very common and debilitating fear anxiety in children with 22q11DS [Scott et al., 2016]. Reduced anatomical connectivity of the hippocampus has also been reported in schizophrenia [Zhou et al., 2008]. The fact that the hippocampus was a significant ROI for Subtype 2, whose hippocampal volumes were similar to the TD group, supports the importance of our cluster analysis method. This is because it shows that a combination of features, rather than a single difference like hippocampal volume, can differentiate subtypes that demonstrate measurable differences in hierarchical brain modularity. Again, the functional implications remain unclear and future studies should investigate the relationship of these differences to psychosis risk, if they are robust enough to be identified in other samples of those with 22q11DS.

The differences between Subtype 3 and the TD group may be associated with the high psychosis-proneness risk that is found in 22q11DS, though, as noted above, standard measures like the Structured Interview for Prodromal Syndromes could not be effectively used in this young 22q11DS sample. It is possible to speculate, however, that Subtype 3 may be at highest risk. This is because the right inferior frontal gyrus (IFG; consisting of the pars orbitalis, pars triangularis, and pars opercularis) has been reported to be the largest region of activity in psychotic individuals during experience of auditory verbal hallucinations [Sommer et al., 2008]. Furthermore, a study using machine learning found that connectivity of the right IFG was one of the most discriminative in differentiating individuals with 22q11DS with and without psychotic symptoms [Scariati et al., 2014]. The right IFG is important for perception of prosody [Hoekert et al., 2010], which is the emotional intonation in speech. Individuals who score high on measures of schizotypy but who are otherwise healthy have reduced gray matter volume in the pars orbitalis compared to individuals low on schizotypy (DeRosse et al., 2015). Similarly, individuals at high familial risk for schizophrenia have reduced gray matter volume of the pars orbitalis (Francis et al., 2012), and a reversed lateralization of volume of this region (i.e., $R > L$). Reversed lateralization of cortical thickness of the IFG has also been reported to be greater in children with 22q211 than TD controls. Volume reduction of the right pars orbitalis has been significantly positively correlated with several language measures (Francis et al., 2012). Unfortunately, this study did not examine prosody; however, Francis et al. noted that these findings were consistent with previous findings of loss of language region asymmetry in schizophrenia, and that some have suggested that it may have a genetic basis (Crow, 2000).

Consistent with our findings of frontotemporal interlobar dysconnectivity, some theoretical models argue that an overactive auditory cortex and a failure of top–down inhibitory control contributes to the genesis of auditory and visual hallucinations [Allen et al., 2008; Dierks et al., 1992; Hugdahl, 2009]. Overactivity of sensory areas could result from an underactivity of cognitive control regions, such as the ventrolateral prefrontal cortex (VLPFC), which is densely connected to the rostral inferior temporal visual

association cortex via the uncinate fasciculus [Barbas, 1988; Carmichael and Price, 1995; Petrides and Pandya, 2002]. Numerous studies have found that the VLPFC, including pars orbitalis and pars triangularis of the IFG, is important for cognitive control [Chavan et al., 2015]. For example, an fMRI study of face-word Stroop tasks [Egner, 2011] found that individual differences in successful conflict-driven adjustments in cognitive control were supported by the right inferior frontal gyrus, which is part of the VLPFC. Furthermore, inhibitory control is clearly impaired in children with 22q11DS [Shapiro et al., 2014].

The differences found in the posteromedial parietal lobes, including the precuneus, are also likely to be important because these regions are crucial for visuo-spatial processing [Cavanna and Trimble, 2006] and numerical calculations [Zago and Tzourio-Mazoyer, 2002], abilities that are impaired in a very high proportion of those with 22q11DS [De Smedt et al., 2006; Simon, 2008; Simon et al., 2005a; Wang et al., 2000]. The posterior cingulate cortex is also involved in spatial attention and forms an important part of the cingulate component of the attention network [Mesulam et al., 2001]. Reduced gray matter and increased fractional anisotropy has been reported in this posterior cingulate/precuneus region in children with 22q11DS compared to TD controls [Simon et al., 2005b]. Reduced surface area has also been reported in the precuneus of individuals with delusional infestation [Hirjak et al., 2017], a monothematic delusional disorder on the psychosis spectrum. Overall, the findings from the PLACE analysis also suggest a frontoparietal interlobar dysconnectivity, at least in 22q11DS Subtypes 2 and 3. Indeed, a dysfunction in frontal and parietal neural circuitry has previously been suggested as a potential mechanism underlying inhibitory impairments in this population [Simon et al., 2005b].

The results of our PLACE analysis are also consistent with a recent connectome study of 22q11DS [Váša et al., 2016]. This study found that connectomes of individuals with 22q11DS had increased characteristic path length and decreased global efficiency, and lower global segregation. The regions driving their global group difference included the hippocampal formation (the entorhinal cortex and hippocampus), in addition to the precentral gyrus (both of which were significantly different in 22q11DS Subtype 2 compared to the TD group in the PLACE analysis) and the precuneus (significant in Subtype 3).

Interestingly, all our significant ROIs for the PLACE analysis were located in the right hemisphere, which is consistent with the right lateralization of auditory verbal hallucinatory activity reported by Sommer et al. [2008] and others [Woodruff et al., 1995], and the degree to which the content of auditory verbal hallucinations was negative in valence [Sommer et al., 2008]. The restriction of significant results to the right hemisphere may also be related to the prevalent spatiotemporal processing impairments in 22q11DS. Our analyses found connective differences in several thalamocortical networks critical to spatiotemporal processing [Kadosh et al., 2007] that are consistent with characteristically impaired visuospatial [Bearden et al., 2001], attentional, and temporal processes in 22q11DS [Simon, 2008]. Furthermore, these suggest functional implications for the 22q11DS midline structural subtypes identified by independent k-means clustering. We present these potential relationships because they form an interesting set of hypotheses requiring direct investigation in future studies.

Finally, the intrinsic geometry analysis further confirmed the above bilateral discussion because it found that connections between the temporal lobes were less integrated in 22q11DS Subtype 3 compared to the TD group. Many studies have reported abnormalities in the temporal lobe in 22q11DS [Eliez et al., 2001; Scariati et al., 2014; van Amelsvoort et al., 2001]. For example, in nonpsychotic youth with 22q11DS, reduced temporal lobe gray matter has been associated with severity of thought problems [Bearden et al., 2004]. Decreased cortical thickness has been reported in individuals with 22q11DS [Schmitt et al., 2015], and widespread decreased temporal lobe white matter in individuals with and without schizophrenia that was related to schizophrenia symptom (PANSS) severity [Alves et al., 2011]. Kates et al. [2011] found that symptom severity over a 3-year follow-up of individuals with 22q11DS was associated with volume loss in several brain regions; however, only temporal lobe gray matter loss and reductions in verbal IQ uniquely predicted severity of positive psychotic symptoms at follow-up, although no individuals had converted to full psychosis. Similarly, Chow et al. [2011] found that among individuals with 22q11DS, those with schizophrenia had significant gray matter volume reductions in the temporal lobes and superior temporal gyri. Findings of reduced temporal gray matter are consistent with those from studies of first-episode schizophrenia [Kasai et al., 2003]. Enlarged Sylvian fissures, perhaps due to delayed development of the opercular regions, have also been reported in children with 22q11DS [Bingham et al., 1997].

Fronto-temporal dysconnectivity has been frequently implicated in schizophrenia and reported in 22q11DS [Ottet et al., 2013]; however, this was in the left hemisphere. Impaired synchrony between the prefrontal cortex and hippocampus has been found in mice modeled with 22q11DS [Sigurdsson et al., 2010] and it was suggested that this impaired synchrony could be an essential component underlying the pathophysiology of schizophrenia and its intermediate phenotype of executive functioning. As mentioned, the children with 22q11DS analyzed in this study were not assessed for schizophrenia spectrum disorder symptomology during their research visit, and given their young age, they would not be expected to reveal many such symptoms. Thus, we hope that subsequent studies attempt to replicate the novel findings presented here using designs that allow for direct testing of associations with intermediate cognitive phenotypes of psychosis risk and direct assessments of symptomology. Should such

relationships be found, then there would be increased confidence that connectomic findings like those presented here are important biomarkers for psychosis-proneness assessed in high-risk groups such as individuals with 22q11DS and those with first degree relatives with a psychotic disorder.

LIMITATIONS

This study has the following limitations. First, due to the relatively small sample size, we unfortunately could not jointly investigate sex and age effect on modularity. However, we computed and compared modularity for 38 subjects versus 44 subjects (<10 years old vs 10∼14 years old; regardless of sex), and confirmed that there was no significant difference. Similarly, a comparison between 39 males and 43 females, regardless of age, revealed no significant difference.

Second, the results of our k-means clustering using midline structures should be replicated to confirm the identified three Subtypes in a larger sample. Also, the cross-sectional nature of our study does not inform us about the longitudinal time course; so in the next phase of our study, we will follow these subjects over time in order to determine whether our connectome findings between different subtypes translate to different clinical trajectories. Last, our structural networks were defined by simply counting the number of fibers connecting two regions of interest, without taking into account the size and/or the surface area of each ROI and the distance between them (however, we note that while alternative strategies have been proposed, to the best of our knowledge, there is currently no consensus in the literature).

CONCLUSIONS

Our results suggest that connectomic analysis can reveal functionally significant within-group differences that might identify outcome risk subtypes, independent of observable differences in regional brain structures. In particular, we observed overall impaired fronto-parietal and fronto-temporal interlobar connectivity in the two most grossly atypical Subtypes of 22q11DS. These network alterations could be state factors that appear with the emergence of schizophrenia, or they could represent endophenotypic biomarkers [Keshavan et al., 2007], or trait vulnerability factors for developing schizophrenia. Studies that measure the connectomes of individuals with 22q11DS are therefore important given the high genetic risk for schizophrenia in this sample.

ACKNOWLEDGMENTS

This work has been partially supported by NIH AG056782 (ADL and LZ), HD042974 (TJS and DJH), MH107108 (TJS) and HD079125 (TJS and DJH).

CONFLICT OF INTEREST STATEMENT

The authors declare that the research was conducted in the absence of any commercial or financial relationships that could be construed as a potential conflict of interest.

REFERENCES

Allen P, Laroi F, McGuire PK, Aleman A (2008): The hallucinating brain: A review of structural and functional neuroimaging studies of hallucinations. Neurosci Biobehav Rev 32:175–191.

Alves FD, Schmitz N, Bloemen O, van der Meer J, Meijer J, Boot E, Nederveen A, de Haan L, Linszen D, van Amelsvoort T (2011): White matter abnormalities in adults with 22q11 deletion syndrome with and without schizophrenia. Schizophr Res 132:75–83.

Andersson JLR, Sotiropoulos SN (2016): An integrated approach to correction for off-resonance effects and subject movement in diffusion MR imaging. NeuroImage 125:1063–1078.

Angkustsiri K, Goodlin-Jones B, Deprey L, Brahmbhatt K, Harris S, Simon TJ (2014): Social impairments in chromosome 22q11.2 deletion syndrome (22q11.2DS): Autism spectrum disorder or a different endophenotype? J Autism Dev Disord 44:739–746.

Angkustsiri K, Leckliter I, Tartaglia N, Beaton EA, Enriquez J, Simon TJ (2012): An examination of the relationship of anxiety and intelligence to adaptive functioning in children with chromosome 22q11.2 deletion syndrome. J Dev Behav Pediatr 33: 713–720.

Avants BB, Epstein CL, Grossman M, Gee JC (2008): Symmetric diffeomorphic image registration with cross-correlation: Evaluating automated labeling of elderly and neurodegenerative brain. Med Image Anal 12:26–41.

Azuma R, Daly EM, Campbell LE, Stevens AF, Deeley Q, Giampietro V, Brammer MJ, Glaser B, Ambery FZ, Morris RG, Williams SCR, Owen MJ, Murphy DGM, Murphy KC (2009): Visuospatial working memory in children and adolescents with 22q11.2 deletion syndrome: An fMRI study. J Neurodev Disord 1:46–60.

Barbas H (1988): Architectonic and connectional organization of ventral and dorsal prefrontal areas in the rhesus monkey. Epilepsia 29:209–210.

Bearden CE, van Erp TG, Monterosso JR, Simon TJ, Glahn DC, Saleh PA, Hill NM, McDonald-McGinn DM, Zackai E, Emannuel BS, Cannon TD (2004): Regional brain abnormalities in 22q11.2 deletion syndrome: Association with cognitive abilities and behavioral symptoms. Neurocase 10:198–206.

Bearden CE, Woodin MF, Wang PP, Moss E, McDonald-McGinn D, Zackai E, Emannuel B, Cannon TD (2001): The neurocognitive phenotype of the 22Q11.2 deletion syndrome: Selective deficit in visual-spatial memory. J Clin Exp Neuropsychol 23: 447–464.

Beaton EA, Qin YF, Nguyen V, Johnson J, Pinter JD, Simon TJ (2010): Increased incidence and size of cavum septum pellucidum in children with chromosome 22q11.2 deletion syndrome. Psychiatry Res Neuroimaging 181:108–113.

Bingham PM, Zimmerman RA, McDonaldMcGinn D, Driscoll D, Emanuel BS, Zackai E (1997): Enlarged Sylvian fissures in infants with interstitial deletion of chromosome 22q11. Am J Med Genet 74:538–543.

Bish JP, Chiodo R, Mattei V, Simon TJ (2007): Domain specific attentional impairments in children with chromosome 22q11.2 deletion syndrome. Brain Cogn 64:265–273.

Campbell LE, Azuma R, Ambery F, Stevens A, Smith A, Morris RG, Murphy DGM, Murphy KC (2010): Executive functions and memory abilities in children with 22q11.2 deletion syndrome. Aust N Z J Psychiatry 44:364–371.

Campbell LE, Daly E, Toal F, Stevens A, Azuma R, Catani M, Ng V, van Amelsvoort T, Chitnis X, Cutter W, Murphy DGM, Murphy KC (2006): Brain and behaviour in children with 22q11.2 deletion syndrome: A volumetric and voxel-based morphometry MRI study. Brain 129:1218–1228.

Carmichael ST, Price JL (1995): Sensory and premotor connections of the orbital and medial prefrontal cortex of macaque monkeys. J Comp Neurol 363:642–664.

Cavanna AE, Trimble MR (2006): The precuneus: A review of its functional anatomy and behavioural correlates. Brain 129: 564–583.

Chavan CF, Mouthon M, Draganski B, van der Zwaag W, Spierer L (2015): Differential patterns of functional and structural plasticity within and between inferior frontal gyri support training-induced improvements in inhibitory control proficiency. Hum Brain Mapp 36:2527–2543.

Chow EW, Ho A, Wei C, Voormolen EH, Crawley AP, Bassett AS (2011): Association of schizophrenia in 22q11.2 deletion syndromw and gray matter volumetric deficits in the superior temporal gyrus. Am J Psychiatry 168:522–529.

Conte G, Ye AQ, Forbes AG, Ajilore O, Leow A (2015): BRAINtrinsic: A virtual reality-compatible tool for exploring intrinsic topologies of the human brain connectome. Brain Inform Health 67–76.

Crow TJ (2000): Invited commentary on: functional anatomy of verbal fluency in people with schizophrenia and those at genetic risk. The genetics of asymmetry and psychosis. Br J Psychiatry 176:61–63.

De Smedt B, Swillen A, Devriendt K, Fryns JP, Verschaffel L, Ghesquiere P (2006): Mathematical disabilities in young primary school children with Velo-Cardio-Facial Syndrome. Genet Couns 17:259–280.

Debbane M, Schaer M, Farhoumand R, Glaser B, Eliez S (2006): Hippocampal volume reduction in 22q11.2 deletion syndrome. Neuropsychologia 44:2360–2365.

DeBoer T, Wu Z, Lee A, Simon TJ (2007): Hippocampal volume reduction in children with chromosome 22q11.2 deletion syndrome is associated with cognitive impairment. Behav Brain Funct 3:9.

Deng Y, Goodrich-Hunsaker NJ, Cabaral M, Amaral DG, Buonocore MH, Harvey D, Kalish K, Carmichael OT, Schumann CM, Lee A, Dougherty RF, Perry LM, Wandell BA, Simon TJ (2015): Disrupted fornix integrity in children with chromosome 22q11.2 deletion syndrome. Psychiatry Res Neuroimaging 232:106–114.

DeRosse P, Nitzburg GC, Ikuta T, Peters BD, Malhotra AK, Szeszko PR (2015): Evidence from structural and diffusion tensor imaging for frontotemporal deficits in psychometric schizotypy. Schizophr Bull 41:104–114.

Desikan RS, Segonne F, Fischl B, Quinn BT, Dickerson BC, Blacker D, Buckner RL, Dale AM, Maguire RP, Hyman BT, Albert MS, Killiany RJ (2006): An automated labeling system for subdividing the human cerebral cortex on MRI scans into gyral based regions of interest. NeuroImage 31:968–980.

Dierks T, Linden DEJ, Jandl M, Formisano E, Goebel R, Lanfermann H, Singer W (1992): Activation of Heschl's gyrus during auditory hallucinations. Neuron 22.

DiGeorge A (1965): A new concept of the cellular basis of immunity. J Pediatr 67:907.

Edelmann L, Pandita RK, Spiteri E, Funke B, Goldberg R, Palanisamy N, Chaganti RSK, Magenis E, Shprintzen RJ, Morrow BE (1999): A common molecular basis for rearrangement disorders on chromosome 22q11. Hum Mol Genet 8:1157–1167.

Egner T (2011): Right ventrolateral prefrontal cortex mediates individual differences in conflict-driven cognitive control. J Cogn Neurosci 23:3903–3913.

Eliez S (2007): Autism in children with 22Q11.2 deletion syndrome. J Am Acad Child Adolesc Psychiatry 46:433–434.

Eliez S, Blasey CM, Schmitt EJ, White CD, Hu D, Reiss AL (2001): Velocardiofacial syndrome: Are structural changes in the temporal and mesial temporal regions related to schizophrenia? Am J Psychiatry 158:447–453.

Eliez S, Schmitt JE, White CD, Reiss AL (2000): Children and adolescents with velocardiofacial syndrome: A volumetric MRI study. Am J Psychiatry 157:409–415.

Feinstein C, Eliez S, Blasey C, Reiss AL (2002): Psychiatric disorders and behavioral problems in children with velocardiofacial syndrome: Usefulness as phenotypic indicators of schizophrenia risk. Biol Psychiatry 51:312–318.

Francis AN, Seidman LJ, Jabbar GA, Mesholam-Gately R, Thermenos HW, Juelich R, Proal AC, Shenton M, Kubicki M, Mathew I, Keshavan M, Delisi LE (2012): Alterations in brain structures underlying language function in young adults at high familial risk for schizophrenia. Schizophr Res 141:65–171.

GadElkarim JJ, Ajilore O, Schonfeld D, Zhan L, Thompson PM, Feusner JD, Kumar A, Altshuler LL, Leow AD (2014): Investigating brain community structure abnormalities in bipolar disorder using path length associated community estimation. Hum Brain Mapp 35:2253–2264.

GadElkarim JJ, Schonfeld D, Ajilore O, Zhan L, Zhang AF, Feusner JD, Thompson PM, Simon TJ, Kumar A, Leow AD (2012): A framework for quantifying node-level community structure group differences in brain connectivity networks. Med Image Comput Comp Assist Interv 15:196–203.

Galarza M, Merlo AB, Ingratta A, Albanese EF, Albanese AM (2004): Cavum septum pellucidum and its increased prevalence in schizophrenia: A neuroembryological classification. J Neuropsychiatr Clin Neurosci 16:41–46.

Gothelf D, Schneider M, Green T, Debbane M, Frisch A, Glaser B, Zilkha H, Schaer M, Weizman A, Eliez S (2013): Risk factors and the evolution of psychosis in 22q11.2 deletion syndrome: A longitudinal 2-site study. J Am Acad Child Adolesc Psychiatry 52:1192–1203.

Grati FR, Gomes DM, Ferreira J, Dupont C, Alesi V, Gouas L, Horelli-Kuitunen N, Choy KW, Garcia-Herrero S, de la Vega AG, Piotrowski K, Genesio R, Queipo G, Malvestiti B, Herve B, Benzacken B, Novelli A, Vago P, Piippo K, Leung TY, Maggi F, Quibel T, Tabet AC, Simoni G, Vialard F (2015): Prevalence of recurrent pathogenic microdeletions and microduplications in over 9500 pregnancies. Prenat Diagn 35: 801–809.

Green T, Gothelf D, Glaser B, Debbane M, Frisch A, Kotler M, Weizman A, Eliez S (2009): Psychiatric disorders and intellectual functioning throughout development in velocardiofacial (22q11.2 Deletion) syndrome. J Am Acad Child Adolesc Psychiatry 48:1060–1068.

Hirjak D, Huber M, Kirchler E, Kubera KM, Karner M, Sambataro F, Freudenmann RW, Wolf RC (2017): Cortical features of distinct developmental trajectories in patients with delusional infestation. Prog Neuropsychopharmacol Biol Psychiatry 76: 72–79.

Hoekert M, Vingerhoets G, Aleman A (2010): Results of a pilot study on the involvement of bilateral inferior frontal gyri in emotional prosody perception: An rTMS study. BMC Neurosci 11:8.

Hugdahl K (2009): "Hearing voices": Auditory hallucinations as failure of top-down control of bottom-up perceptual processes. Scand J Psychol 50:553–560.

Jolin EM, Weller RA, Weller EB (2012): Occurrence of affective disorders compared to other psychiatric disorders in children and adolescents with 22q11.2 deletion syndrome. J Affect Disord 136:222–228.

Kadosh RC, Kadosh KC, Linden DEJ, Gevers W, Berger A, Henik A (2007): The brain locus of interaction between number and size: A combined functional magnetic resonance Imaging and event-related potential study. J Cogn Neurosci 19:957–970.

Karayiorgou M, Simon TJ, Gogos JA (2010): 22q11.2 microdeletions: Linking DNA structural variation to brain dysfunction and schizophrenia. Nat Rev Neurosci 11:402–416.

Kasai K, Shenton ME, Salisbury DF, Hirayasu Y, Lee CU, Cizewski AA, Yurgelun-Todd D, Kikinis R, Jolesz FA, McCarley RW (2003): Progressive decrease of left superior temporal gyrus gray matter volume in patients with first-episode schizophrenia. Am J Psychiatry 160:156–164.

Kates WR, Antshel KM, Faraone SV, Fremont WP, Higgins AM, Shprintzen RJ, Botti JA, Kelchner L, McCarthy C (2011): Neuroanatomic predictors to prodromal psychosis in velocardiofacial syndrome (22q11.2 Deletion Syndrome): A longitudinal study. Biol Psychiatry 69:945–952.

Kates WR, Burnette CP, Jabs EW, Rutberg J, Murphy AM, Grados M, Geraghty M, Kaufmann WE, Pearlson GD (2001): Regional cortical white matter reductions in velocardiofacial syndrome: A volumetric MRI analysis. Biol Psychiatry 49:677–684.

Kates WR, Olszewski AK, Gnirke M, Kikinis Z, Nelson J, Antshel KM, Fremont W, Radoeva PD, Middleton FA, Shenton ME, Coman IL (2015): White matter microstructural abnormalities of the cingulum bundle in youths with 22q11.2 deletion syndrome: Associations with medication, neuropsychological function, and prodromal symptoms of psychosis. Schizophr Res 161:76–84.

Keshavan MS, Prasad KM, Pearlson G (2007): Are brain structural abnormalities useful as endophenotypes in schizophrenia? Int Rev Psychiatry (Abingdon, England) 19:397–406.

Klein A, Andersson J, Ardekani BA, Ashburner J, Avants B, Chiang MC, Christensen GE, Collins DL, Gee J, Hellier P, Song JH, Jenkinson M, Lepage C, Rueckert D, Thompson P, Vercauteren T, Woods RP, Mann JJ, Parsey RV (2009): Evaluation of 14 nonlinear deformation algorithms applied to human brain MRI registration. NeuroImage 46:786–802.

Machado AMC, Simon TJ, Nguyen V, McDonald-McGinn DM, Zackai EH, Gee JC (2007): Corpus callosum morphology and ventricular size in chromosome 22q11.2 deletion syndrome. Brain Res 1131:197–210.

McCabe K, Rich D, Loughland CM, Schall U, Campbell LE (2011): Visual scanpath abnormalities in 22q11.2 deletion syndrome: Is this a face specific deficit? Psychiatry Res 189:292–298.

McDonald-McGinn DM, Sullivan KE, Marino B, Philip N, Swillen A, Vorstman JAS, Zackai EH, Emannuel BS, Vermeesch JR, Morrow BE, Scambler PJ, Bassett AS (2015): 22q11.2 deletion syndrome. Nat Rev Dis Primers 15071.

McGuffin P, Owen MJ, Farmer AE (1995): Genetic basis of schizophrenia. Lancet 346:678–682.

Mesulam MM, Nobre AC, Kim YH, Parrish TB, Gitelman DR (2001): Heterogeneity of cingulate contributions to spatial attention. NeuroImage 13:1065–1072.

Mori S, Crain BJ, Chacko VP, van Zijl PCM (1999): Three-dimensional tracking of axonal projections in the brain by magnetic resonance imaging. Ann Neurol 45:265–269.

Murphy KC, Jones LA, Owen MJ (1999): High rates of schizophrenia in adults with velo-cardio-facial syndrome. Arch Gen Psychiatry 56:940–945.

Nopoulos P, Krie A, Andreasen NC (2000): Enlarged cavum septi pellucidi in patients with schizophrenia. Clinical and cognitive correlates. J Neuropsychiatr Clin Neurosci 12:344–349.

Ottet MC, Schaer M, Cammoun L, Schneider M, Debbane M, Thiran JP, Eliez S (2013): Reduced fronto-temporal and limbic connectivity in the 22q11.2 deletion syndrome: Vulnerability markers for developing schizophrenia? PLoS One 8:8.

Petrides M, Pandya DN (2002): Comparative cytoarchitectonic analysis of the human and the macaque ventrolateral prefrontal cortex and corticocortical connection patterns in the monkey. Eur J Neurosci 16:291–310.

Reynolds C, Kamphaus R (2004) Behavior Assessment System for Children, Second Edition (BASC- 2) Handout. AGS Publishing, 4201 Woodland Road, Circle Pines, MN 55014-1796: American Guidance Service.

Rubinov M, Sporns O (2010): Complex network measures of brain connectivity: Uses and interpretations. NeuroImage 52: 1059–1069.

Rutter M, Bailey A, Lord C, Berument S (2003): Social Communication Questionnaire (SCQ). Los Angeles, CA: Western Psychological Services.

Scariati E, Schaer M, Richiardi J, Schneider M, Debbane M, Van De Ville D, Eliez S (2014): Identifying 22q11.2 deletion syndrome and psychosis using resting-state connectivity patterns. Brain Topogr 27:808–821.

Schmitt JE, Vandekar S, Yi J, Calkins ME, Ruparel K, Roalf DR, Whinna D, Souders MC, Satterwaite TD, Prabhakaran K, McDonald-McGinn DM, Zackai EH, Gur RC, Emanuel BS, Gur RE (2015): Aberrant cortical morphometry in the 22q11.2 deletion syndrome. Biol Psychiatry 78:135–143.

Schmitt JE, Yi JJ, Roalf DR, Loevner LA, Ruparel K, Whinna D, Souders MC, McDonald-McGinn DM, Yodh E, Vandekar S, Zackai EH, Gur RC, Emanuel BS, Gur RE (2014): Incidental radiologic findings in the 22q11.2 deletion syndrome. Am J Neuroradiol 35:2186–2191.

Schneider M, Debbane M, Bassett AS, Chow EWC, Fung WLA, van den Bree MBM, Owen M, Murphy KC, Niarchou M, Kates WR, Antshel KM, Fremont W, McDonald-McGinn DM, Gur RE, Zackai EH, Vorstman J, Duijff SN, Klaassen PWJ, Swillen A, Gothelf D, Green T, Weizman A, Van Amelsvoort T, Evers L, Boot E, Shashi V, Hooper SR, Bearden CE, Jalbrzikowski M, Armando M, Vicari S, Murphy DG, Ousley O, Campbell LE, Simon TJ, Eliez S, Int Consortium Brain Behav q (2014): Psychiatric disorders from childhood to adulthood in 22q11.2 deletion syndrome: Results from the International Consortium on Brain and Behavior in 22q11.2 Deletion Syndrome. Am J Psychiatry 171:627–639.

Scott JA, Goodrich-Hunsaker N, Kalish K, Lee A, Hunsaker MR, Schumann CM, Carmichael OT, Simon TJ (2016): The hippocampi of children with chromosome 22q11.2 deletion syndrome have localized anterior alterations that predict severity of anxiety. J Psychiatry Neurosci 41:203–213.

Shaikh TH, Kurahashi H, Saitta SC, O'Hare AM, Hu P, Roe BA, Driscoll DA, McDonald-McGinn DM, Zackai EH, Budarf ML, Emanuel BS (2000): Chromosome 22-specific low copy repeats and the 22q11.2 deletion syndrome: Genomic organization and deletion endpoint analysis. Hum Mol Genet 9:489–501.

Shapiro HM, Tassone F, Choudhary NS, Simon TJ (2014): The development of cognitive control in children with chromosome 22q11.2 deletion syndrome. Front Psychol 5:14.

Shashi V, Francis A, Hooper SR, Kranz PG, Zapadka M, Schoch K, Ip E, Tandon N, Howard TD, Keshavan MS (2012): Increased corpus callosum volume in children with chromosome 22q11.2 deletion syndrome is associated with neurocognitive deficits and genetic polymorphisms. Eur J Hum Genet 20:1051–1057.

Shashi V, Muddasani S, Santos CC, Berry MN, Kwapil TR, Lewandowski E, Keshavan MS (2004): Abnormalities of the corpus callosum in nonpsychotic children with chromosome 22q11 deletion syndrome. NeuroImage 21:1399–1406.

Shenton ME, Dickey CC, Frumin M, McCarley RW (2001): A review of MRI findings in schizophrenia. Schizophr Res 49: 1–52.

Shprintzen RJ (2000): Velo-cardio-facial syndrome: A distinctive behavioral phenotype. Ment Retard Dev Disabil Res Rev 6: 142–147.

Shprintzen RJ (2008): Velo-cardio-facial syndrome: 30 Years of study. Dev Disabil Res Rev 14:3–10.

Shprintzen RJ, Goldberg RB, Lewin ML, Sidoti EJ, Berkman MD, Argamaso RV, Young D (1978): New syndrome involving cleft-palate, cardiac anomalies, typical facies, and learning disabilities: Velo-cardio-facial syndrome. Cleft Palate J 15:56–62.

Sigurdsson T, Stark KL, Karayiorgou M, Gogos JA, Gordon JA (2010): Impaired hippocampal-prefrontal synchrony in a genetic mouse model of schizophrenia. Nature 464:763–U139.

Simon TJ (2008): A new account of the neurocognitive foundations of impairments in space, time, and number processing in children with chromosome 22q11.2 deletion syndrome. Dev Disabil Res Rev 14:52–58.

Simon TJ, Bearden CE, Mc-Ginn DM, Zackai E (2005a): Visuospatial and numerical cognitive deficits in children with chromosome 22q11.2 deletion syndrome. Cortex 41:145–155.

Simon TJ, Bish JP, Bearden CE, Ding LJ, Ferrante S, Nguyen V, Gee JC, McDonald-McGinn DM, Zackai EH, Emanuel BS (2005b): A multilevel analysis of cognitive dysfunction and psychopathology associated with chromosome 22q 11.2 deletion syndrome in children. Dev Psychopathol 17:753–784.

Simon TJ, Ding LJ, Bish JP, McDonald-McGinn DM, Zackai EH, Gee J (2005c): Volumetric, connective, and morphologic changes in the brains of children with chromosome 22q11.2 deletion syndrome: An integrative study. NeuroImage 25:169–180.

Simon TJ, Durdle C, Garner J, Popa A, Hunsaker N, Hunsaker MR, Schumann C, Lee A, Kalish K, Carmichael O, Coronado R, Harvey D (2016): Three distinct brain structure patterns as potential biomarkers for behavioral and psychiatric outcomes in chromosome 22q11.2 deletion syndrome. Presented at Society for Biological Psychiatry Conference, Atlanta, GA.

Smith SM (2002): Fast robust automated brain extraction. Hum Brain Mapp 17:143–155.

Sommer IEC, Diederen KMJ, Blom J-D, Willems A, Kushnan L, Slotema K, Boks MPM, Daalman K, Hoek HW, Neggers SFW, Kahn RS (2008): Auditory verbal hallucinations predominantly activate the right inferior frontal area. Brain 131:3169–3177.

Spence S (1999): Spence Children's Anxiety Scale (Parent Version). Brisbane: University of Queensland.

Swanson J, Nolan E, Pelham W (1992): The SNAP-IV Rating Scale. http://wwwadhdnet/snap-iv-formpdf.

Taha AA, Hanbury A (2015): An efficient algorithm for calculating the exact Hausdorff distance. IEEE Trans Pattern Anal Mach Intell 37:2153–2163.

Tan GM, Arnone D, McIntosh AM, Ebmeier KP (2009): Meta-analysis of magnetic resonance imaging studies in chromosome 22q11.2 deletion syndrome (velocardiofacial syndrome). Schizophr Res 115:173–181.

Tang SX, Yi JJ, Calkins ME, Whinna DA, Kohler CG, Souders MC, McDonald-McGinn DM, Zackai EH, Emanuel BS, Gur RC, Gur RE (2014): Psychiatric disorders in 22q11.2 deletion syndrome are prevalent but undertreated. Psychol Med 44:1267–1277.

Van Aken K, Swillen A, Beirinckx M, Janssens L, Caeyenberghs K, Smits-Engelsman B (2010): Prospective control abilities during visuo-manual tracking in children with 22q11.2 Deletion syndrome compared to age- and IQ-matched controls. Res Dev Disabil 31:634–641.

van Amelsvoort T, Daly E, Robertson D, Suckling J, Ng V, Critchley H, Owen MJ, Henry J, Murphy KC, Murphy DGM (2001): Structural brain abnormalities associated with deletion at chromosome 22q11: Quantitative neuroimaging study of adults with velo-cardio-facial syndrome. Br J Psychiatry 178: 412–419.

Váša F, Griffa A, Scariati E, Schaer M, Urben S, Eliez S, Hagmann P (2016): An affected core drives network integration deficits of the structural connectome in 22q11.2 deletion syndrome. NeuroImage Clin 10:239–249.

Vorstman JAS, Morcus MEJ, Duijff SN, Klaassen PWJ, Heineman-de Boer JA, Beemer FA, Swaab H, Kahn RS, van Engeland H (2006): The 22q11.2 deletion in children: High rate of autistic disorders and early onset of psychotic symptoms. J Am Acad Child Adolesc Psychiatry 45:1104–1113.

Wang PP, Woodin MF, Kreps-Falk R, Moss EM (2000): Research on behavioral phenotypes: Velocardiofacial syndrome (deletion 22q11.2). Dev Med Child Neurol 42:422–427.

Wong LM, Riggins T, Harvey D, Cabaral M, Simon TJ (2014): Children with chromosome 22q11.2 deletion syndrome exhibit impaired spatial working memory. AJIDD Am J Intellect Dev Disabil 119:115–132.

Woodruff P, Brammer M, Mellers J, Wright I, Bullmore E, Williams S (1995): Auditory hallucinations and perception of external speech. Lancet 346:1035–1035.

Ye AQ, Zhan L, Conrin S, GadElKarim J, Zhang AF, Yang SL, Feusner JD, Kumar A, Ajilore O, Leow A (2015): Measuring embeddedness: Hierarchical scale-dependent information exchange efficiency of the human brain connectome. Hum Brain Mapp 36:3653–3665.

Zago L, Tzourio-Mazoyer N (2002): Distinguishing visuospatial working memory and complex mental calculation areas within the parietal lobes. Neurosci Lett 331:45–49.

Zhan L, Zhou JY, Wang YL, Jin Y, Jahanshad N, Prasad G, Nir TM, Leonardo CD, Ye JP, Thompson PM, Alzheimer's Dis Neuroimaging I (2015): Comparison of nine tractography algorithms for detecting abnormal structural brain networks in Alzheimer's disease. Front Aging Neurosci 7:19.

Zhou YA, Shu N, Liu Y, Song M, Hao YH, Liu HH, Yu CS, Liu ZN, Jiang TZ (2008): Altered resting-state functional connectivity and anatomical connectivity of hippocampus in schizophrenia. Schizophr Res 100:120–132.